Design and Characterization of a Fringing Field Capacitive Soil Moisture Sensor

Manash Protim Goswami, Babak Montazer, and Utpal Sarma, *Member, IEEE*

***Abstract*— This paper addresses the optimization and implementation of a fringing field capacitive soil moisture sensor using the printed circuit board technology. It includes the analysis of a novel configuration of an interdigital sensor for measuring soil moisture with two existing configurations. The optimized designs were simulated by using a 3-D finite-element method and fabricated by using a copper clad board. The performance of the fabricated sensors was evaluated using four soil samples collected from different locations. The observations were compared with the standard gravimetric method to evaluate the soil water content of the samples. The characterization method and the results of the whole sensing system are discussed in terms of calibration, dynamic test, and repeatability.**

***Index Terms*— Capacitive sensor, fringing field, interdigital sensor, printed circuits, simulation, soil moisture.**

I. Introduction

SOIL moisture is a crucial parameter in the fields of agricultural, geotechnical, hydrological, and environmental engineering. For precision agriculture, the scheduling of irrigation is highly dependent on soil moisture content and plant environment. Understanding the physical behavior of soil water content started with Briggs and McLane in 1897, which was later carried forward by Buckingham, Gardener and Richards [1], [2]. These works provided a conceptual partitioning of soil water content: gravitational water, capillary water, and hygroscopic water. The gravitational water drains away due to the gravitational force, and the capillary water has the properties of capillary action. However, the hygroscopic water cannot drain because of either of these forces. The gravitational water drains out from soil within 2–3 days after rain. Therefore, the capillary water and hygroscopic water are the two main components of the water content of natural soils.

Over the last century, researchers have been continuing to develop various techniques to measure soil water content. However, designing a robust, low-cost, reliable, and real-time measuring soil moisture sensor is still a challenging task. There are several techniques for measuring soil moisture: thermogravimetric, soil resistivity, capacitance, time-domain reflectometry, frequency-domain reflectometry, and neutron scattering.

Manuscript received March 8, 2018; revised June 26, 2018; accepted June 27, 2018. The Associate Editor coordinating the review process was Dr. Samir Trabelsi. *(Corresponding author: Manash Protim Goswami.)*

The authors are with the Department of Instrumentation and USIC, Gauhati University, Guwahati 781014, India (e-mail: manashgoswami@gauhati.ac.in).

Color versions of one or more of the figures in this paper are available online at http://ieeexplore.ieee.org.

Digital Object Identifier 10.1109/TIM.2018.2855538

The thermogravimetric method is the well-known method developed so far and used as the standard method for calibrating soil moisture [3], [4]. However, this test can be performed only in the laboratory and is limited by the difficulty in the removal of soil samples, nonrepeatability of the tests, and extremely time-consuming methods.

Among the modern techniques of measuring soil moisture, time-domain reflectometry is a widely used method. Here, pulses are sent through the soil along a parallel waveguide made of two stainless steel rods as probes, and the delay time between the incident and reflected electromagnetic pulses is calculated [5]–[7]. This method is not cost-effective and is unsuitable for application in highly saline and wet soils.

There are many advanced techniques such as ground-penetrating radar [8], microelectromechanical systems [9], polymer-based microsensor [10], thermal dissipation block [11], heat flux sensor [12], tensiometric [13], [14], optical techniques [15], [16], acoustic continuous-wave method [17], near-infrared reflectance sensor [18], and single-probe heat pulse [19]. Among all these techniques, the measurement of dielectric properties, such as time-domain reflectometry, frequency-domain reflectometry, capacitance measurements, and impedance measurements, is widely used techniques.

Capacitive sensing is a dominant technique for soil moisture measurement. The design of capacitive sensors for such applications by shape optimization is of research interest. Thomas [20] measured the fringing capacitance of a designed probe with coplanar electrodes operated in a very high-frequency range. This paper showed a linear relationship between the moisture and the fringing capacitance for 0%–10% soil moisture content and a linear function of the logarithm of fringing capacitance with 5%–45% soil moisture content. Eller and Denoth [21] designed a capacitive sensor with fork-like geometry and measured the impedance with a twin T-bridge for natural soils. The work was a comparative study with the thermogravimetric method and time-domain reflectometry and led to a satisfactory result. Apart from these attempts, Bell *et al.* [22] designed an annular electrode and Ungar *et al.*[23] developed a cylindrical probe for impedance measurement. The interdigital sensor concept is now widely used for soil moisture measurement. With advances in the printed circuit board (PCB) technology, it is now easier to develop this kind of sensor for various applications. In 2011, Dean *et al.* [24] developed a fringing field sensor for soil moisture measurement using the PCB technology. They evaluated the soil moisture content of clay soil samples with the prototype sensor they designed. Modeling the optimal

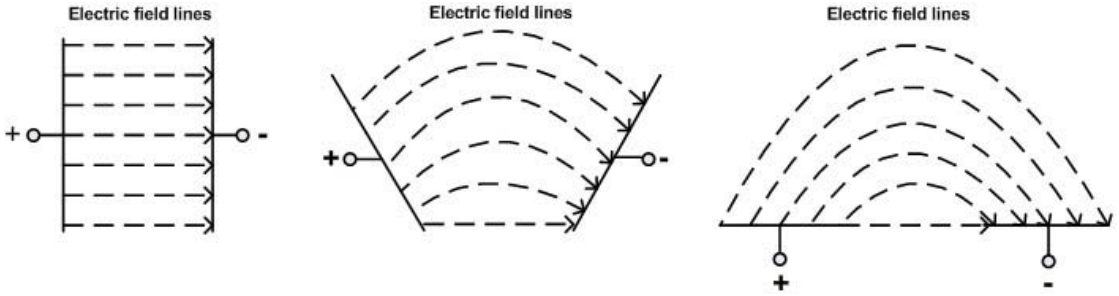

Fig. 1. Electric field lines of capacitors.

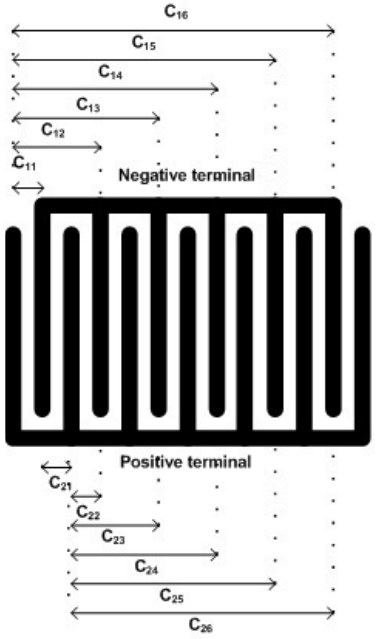

Fig. 2. Interdigital sensor pattern.

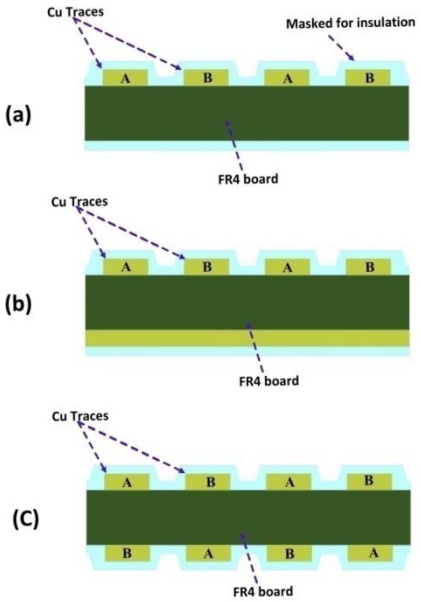

Fig. 3. 2-D illustration of the sensor configurations (a) Model 1, (b) Model 2, and (c) Model 3.

probing frequency, the shape, and the electrical impedance to the humidity of an interdigital sensor for soil moisture measurement has been done by Markevicius *et al.* [25]. Mizuguchi *et al.* [26] have also found a satisfactory result for soil moisture measurement using fringing field capacitive sensors.

Although different works of interdigital capacitive sensor design were reported earlier, a complete analytical model has not yet been computed. As suggested by Mizuguchi *et al.* [26] due to its intrinsic nonlinear characteristic, simulation results are considered instead of an analytical model for sensor design. For designing an interdigital sensor, mainly three design parameters should be accounted for: 1) thickness of the electrodes; 2) separation of two adjacent electrodes; and 3) thickness of the base material. In this paper, after considering all these three parameters, the interdigital sensor designs proposed by Dean *et al.* [24] were simulated. One more configuration is included in this paper to enhance the influence area of the sensor, and hence the sensitivity of the sensor. All three designs were simulated, fabricated, and characterized. The simulation and experimental result analysis, along with a comparison of the three design configurations of the sensors, are presented in this paper. Repeatability tests and dynamic tests for the sensors are also discussed.

II. Methods and Materials

The fringing field capacitive sensor is a dominant field for various sensing applications such as water-level measurement [27], soil water content measurement [24], [26], moisture content of various agricultural commodities [28], and moisture content of wood pallets [29]. As water has a high relative permittivity, it provides a considerable change in capacitance by interacting with the interdigital capacitive sensors. The theory behind the interdigital capacitive sensor, the simulation of designs, the fabrication of sensors, and the signal conditioning is briefly discussed in Section II-A–D.

A. Interdigital Fringing Field Capacitive Sensor

A fringing field capacitor is a capacitor with multiple capacitive plates on the same plane, arranged in an interpenetrating comb pattern [30]. The operating principle of a planar interdigital sensor is based on the same principle as that of a parallel-plate capacitor, where one side of the electrodes is exposed to the materials being tested, as shown in Fig. 1. Therefore, it can be considered as a number of capacitors arranged in a parallel manner with n numbers electrodes, as shown in Fig. 2.

From Fig. 2, for the first positive electrode, capacitance will be $C_{11}, C_{12}, C_{13}, C_{14}, \ldots\ldots\ldots, C_{1n}$ for $1, 2, 3, 4 \ldots, n$ negative electrodes, respectively; for the second positive elec-

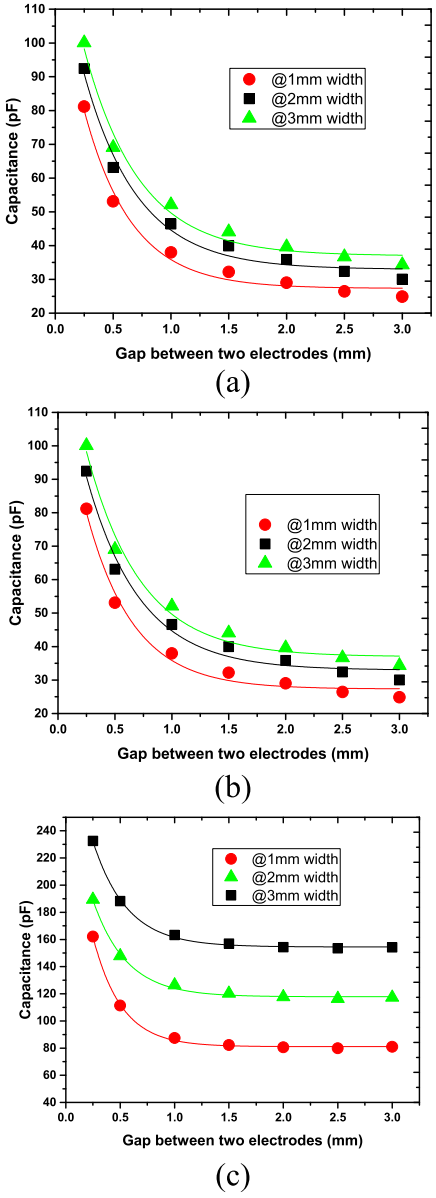

Fig. 4. Capacitance change resulting from electrodes separation in (a) Model 1, (b) Model 2, and (c) Model 3.

trode, capacitance will be $C_{21}, C_{22}, C_{23}, C_{24}, \ldots\ldots\ldots, C_{2n}$ for $1, 2, 3, 4 \ldots, n$ negative electrodes, respectively; and similarly, for the "m" positive electrode, capacitance will be $C_{m1}, C_{m2}, C_{m3}, C_{m4}, \ldots\ldots\ldots, C_{mn}$ for $1, 2, 3, 4 \ldots, n$ negative electrodes, respectively. Thus, the equivalent capacitance of the electrodes is as follows:

$$\left.\begin{aligned} C_{1(\mathrm{eq})} &= C_{11} + C_{12} + C_{13} \\ &\quad + \cdots\cdots\cdots\cdots\cdots\cdots + C_{1n} \\ C_{2(\mathrm{eq})} &= C_{21} + C_{22} + C_{23} \\ &\quad + \cdots\cdots\cdots\cdots\cdots\cdots + C_{2n} \\ C_{3(\mathrm{eq})} &= C_{31} + C_{32} + C_{33} \\ &\quad + \cdots\cdots\cdots\cdots\cdots\cdots + C_{3n} \\ &\vdots \\ C_{m(\mathrm{eq})} &= C_{m1} + C_{m2} + C_{m3} \\ &\quad + \cdots\cdots\cdots\cdots\cdots\cdots + C_{mn} \end{aligned}\right\}. \quad (1)$$

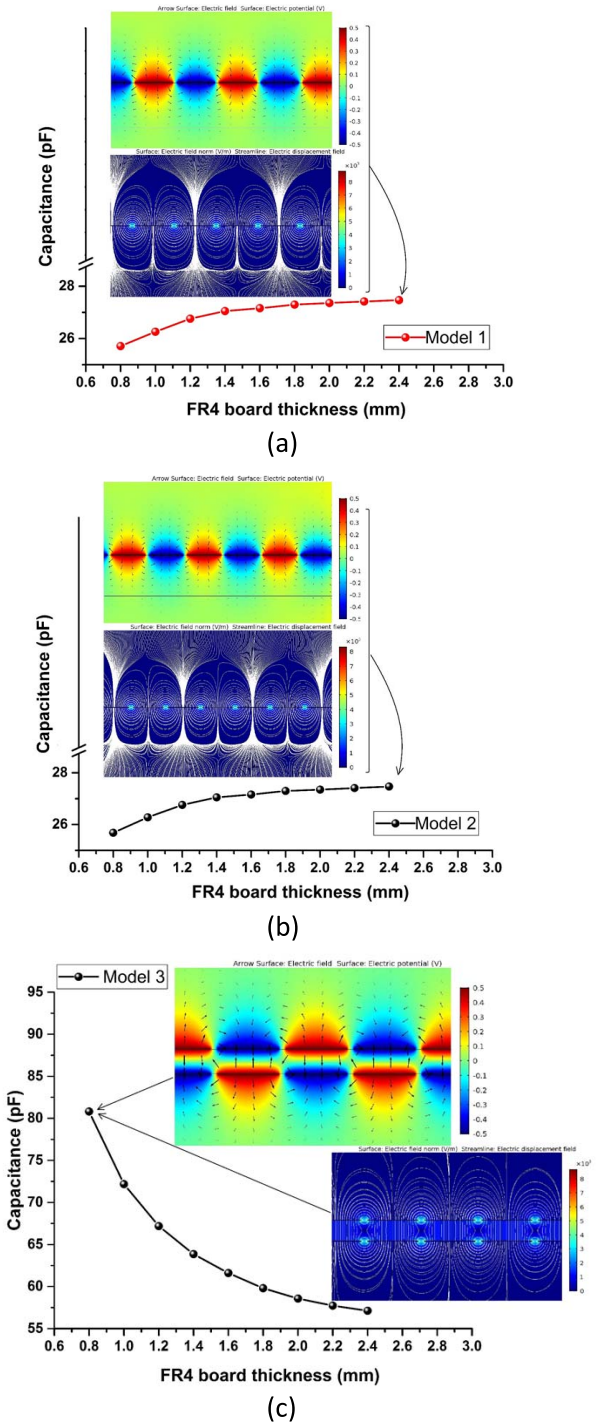

Fig. 5. Change of capacitance with FR4 board thickness in (a) Model 1, (b) Model 2, and (c) Model 3.

Therefore, the total capacitance of the sensor is

$$C_{\mathrm{Total}} = C_{1(\mathrm{eq})} + C_{2(\mathrm{eq})} + C_{3(\mathrm{eq})} + \cdots\cdots\cdots\cdots\cdots\cdots + C_{m(\mathrm{eq})}. \quad (2)$$

The total capacitance of the sensor depends on the electrodes' geometry, the thickness of the electrodes, the distance between two electrodes, the number of electrodes of the sensor, and the material under test.

TABLE I
CHARACTERISTICS OF THE SENSORS OBTAINED FROM LINEAR FITTING

Sensor	Goodness of fit (R^2)	Intercepts	Slopes
Model 1	0.99	65.257	15.478
Model 2	0.99	65.152	15.429
Model 3	1	168.541	34.851

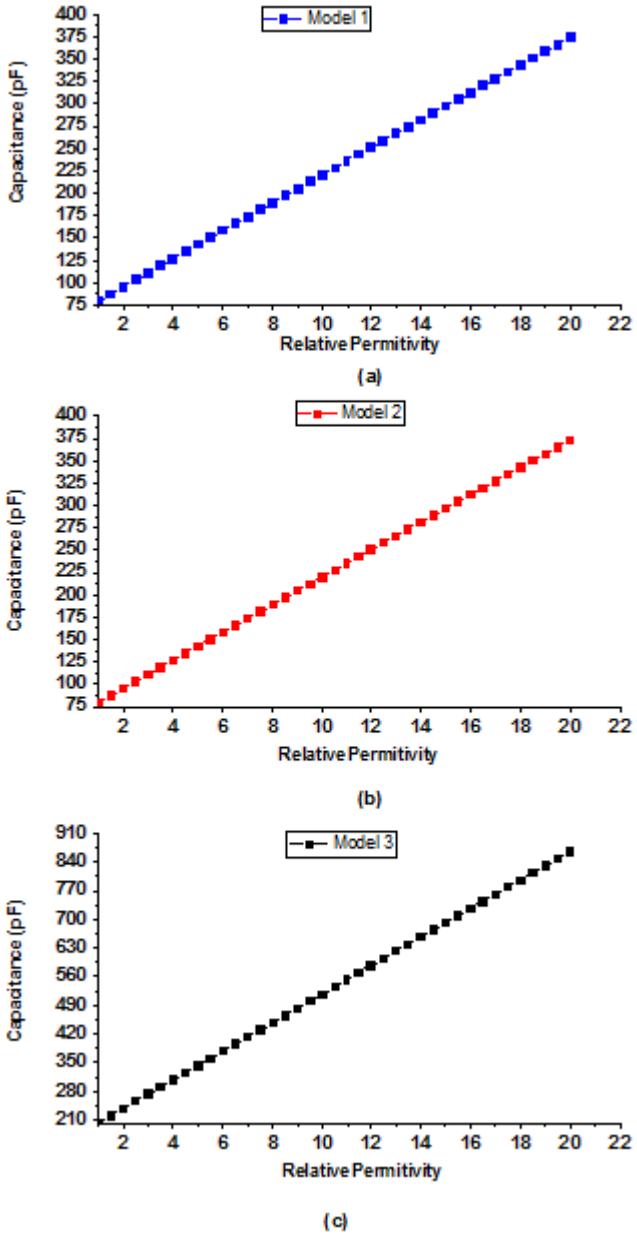

Fig. 6. Change in capacitance with the relative permittivity of the material under test for (a) Model 1, (b) Model 2, and (c) Model 3.

TABLE II
LOCATIONS OF THE SAMPLE COLLECTION AREA

Sample Name	Location
A	26°08'50.5"N 91°39'13.2"E
B	26°08'57.0"N 91°39'04.0"E
C	26°09'49.1"N 91°38'46.5"E
D	26°09'41.3"N 91°38'37.7"E

B. Simulation of the Model

The finite-element method (FEM) is widely used for modeling interdigital capacitive sensors [30]. A 3-D FEM was used to analyze the optimal configuration of an interdigital sensor for soil moisture measurement in this paper. Design considerations for modeling the sensors were the thickness of the electrodes, the separation between two adjacent electrodes, and the thickness of the FR4 material for three different configurations of electrodes. The basic design of the sensor is shown in Fig. 3(a), where the electrodes were fabricated from the copper layer on the top side of the FR4 board (conventional PCB) as proposed by Dean *et al.* [24]. The results obtained by changing the distance between the two electrodes of the sensor for three different thicknesses are shown in Fig. 4(a). It was observed that the capacitance increases by decreasing the distance between the two electrodes and increasing the thickness of the electrodes. If a continuous layer of copper is left on the other side of the FR4 board [configuration as shown in Fig. 3(b)], the result remains the same as shown in Fig. 4(b). As suggested by da Costa *et al.* [31], this continuous copper layer on the opposite side of the electrodes is important for minimizing the change in the capacitance of the sensor due to the presence of water on the backside of the fringing fields. Mamishev *et al.* [32] have mentioned that the dual-sided access to this type of sensors has the advantage of enabling larger, easily measurable capacitances and, more importantly, a uniform field distribution. Accordingly, as shown in Fig. 3(c), the sensor was further modified by fabricating copper traces as electrodes on both the sides of the FR4 board. This step doubled the effective capacitance, as shown in Fig. 4(c). The first configuration is referred to as Model 1 in the later sections, while the second and third configurations are referred to as Models 2 and 3.

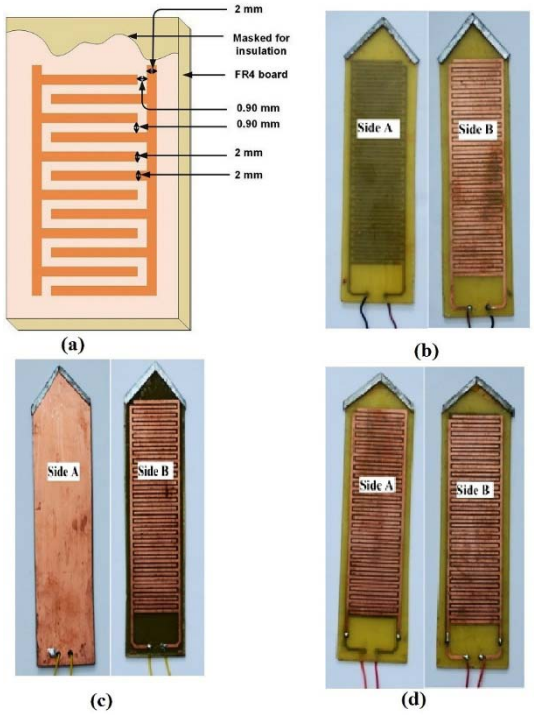

Fig. 7. (a) Interdigitated electrode shape. (b) Model 1. (c) Model 2. (d) Model 3.

Fig. 5 shows the capacitance of the three models versus the FR4 board thickness and their electric field distributions. If the

TABLE III
CHEMICAL ANALYSIS OF THE SOIL SAMPLES (ALL VALUES ARE IN WEIGHT PERCENT)

Elements	SiO_2	Al_2O_3	Fe_2O_3	MnO	MgO	CaO	Na_2O	K_2O	TiO_2	P_2O_5
Sample A	60.08	20.68	7.75	0.195	0.16	1.02	2.22	2.99	1.35	0.11
Sample B	53.05	12.87	3.6	0.062	0.12	0.61	2.18	1.21	0.64	0.04
Sample C	58.34	17.07	6.97	0.147	1.47	7.81	2.60	3.71	1.15	0.63
Sample D	56.80	14.87	6.33	0.132	1.68	7.15	2.62	2.68	1.04	0.79

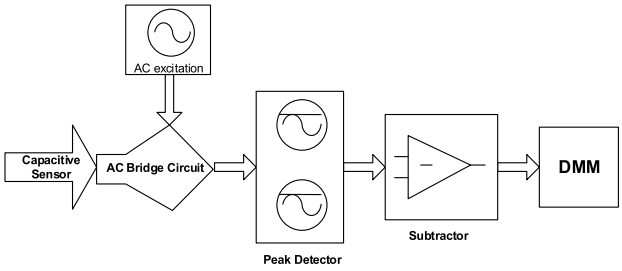

Fig. 8. Block diagram of the soil moisture sensor system.

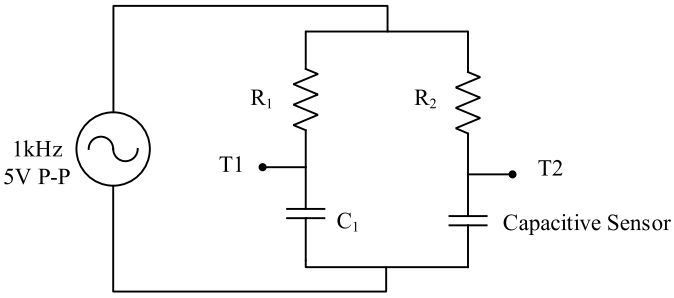

Fig. 9. Bridge circuit for impedance measurement.

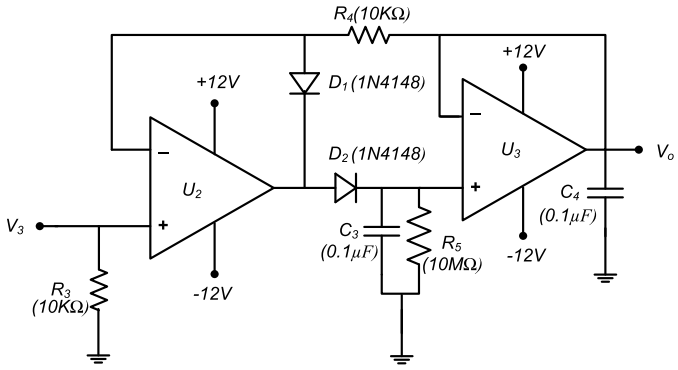

Fig. 10. Schematic of the peak detector circuit.

thickness of the FR4 board is increased, then the capacitance of Models 1 and 2 also increases as shown in Fig. 5(a) and (b), whereas the capacitance of Model 3 decreases as shown in Fig. 5(c). Simulation was done for all models by placing 13 electrodes on either side, with the electrode thickness kept at 2 mm and the separation maintained at 0.25 mm.

Simulation was done for all the three models with different relative permittivities, the result of which is shown in Fig. 6. As is evident from Table I, Model 3 has a better sensitivity, whereas Models 1 and 2 also show similar results.

C. Sensor Fabrication

The PCB technology is a cost-effective method of easily fabricating an interpenetrating comb pattern. An interpenetrating comb pattern electrode was accordingly designed in the PCB as copper traces to give a fringe capacitance. Three prototype models were configured as shown in Fig. 7 and named Models 1–3, respectively. As shown in Fig. 7(b), the sensor was fabricated in such a way that copper traces remain on one side of the FR4 board in shape resembling interpenetrating combs and was designated as Model 1. In Fig. 7(c), one side of the FR4 board was covered by copper traces in an interpenetrating comb shape and the other side was covered with copper, and was designated as Model 2. The two sides of the FR4 board were covered by the interpenetrating comb pattern in Model 3 as shown in Fig. 7(d). In all the cases, the thickness of the FR4 board was 1.5 mm and the thickness of the copper layer was 35 μm. The total number of capacitive electrodes was 51 out of which 26 electrodes were connected on one side and the remaining 25 electrodes were connected on the other side. The gap between any two adjacent electrodes was 0.90 mm, the width of each plate was 2 mm, and the total length of the sensor was 150 mm (of which the sensing part was 147 mm). The copper traces were masked with quick-drying lacquer spray (Acrylic Epoxy) with an average thickness of about 52.5 μm. All the thickness was measured by a digital slide caliper with an accuracy of 1 μm.

D. Signal Conditioning Circuit

There are several techniques for measuring capacitance. A fringing field capacitive sensor is a combination of capacitance with parallel resistance. The impedance bridge method is suitable for capacitive measurement with the help of which the output signal can be conditioned efficiently [33]. A block diagram of the signal conditioning circuit for the capacitive soil moisture sensor is shown in Fig. 8. The bridge was excited by means of an ac excitation signal of low frequency (1 kHz and 5-V peak to peak), as shown in Fig. 9.

The output at the two test points (T1 and T2 in Fig. 9) had a difference in the phase and the amplitude. To sense the soil moisture with this sensor, both the amplitude difference and the phase difference can be used. The easiest method

TABLE IV
RESPONSE OF THE SENSORS TO THE SOIL SAMPLES

Samples Name	Sensors	Intercept	Slope	Goodness of fit(R^2)
Soil sample A	Model 1	39.154	51.404	0.962
	Model 2	111.337	25.124	0.971
	Model 3	53.674	86.52	0.965
Soil sample B	Model 1	66.975	48.601	0.966
	Model 2	123.002	24.24	0.982
	Model 3	138.44	76.70	0.971
Soil sample C	Model 1	144.72	20.19	0.994
	Model 2	146.21	14.12	0.996
	Model 3	275.25	25.679	0.997
Soil sample D	Model 1	115.26	20.18	0.997
	Model 2	161.5	14.27	0.991
	Model 3	188.86	30.33	0.978

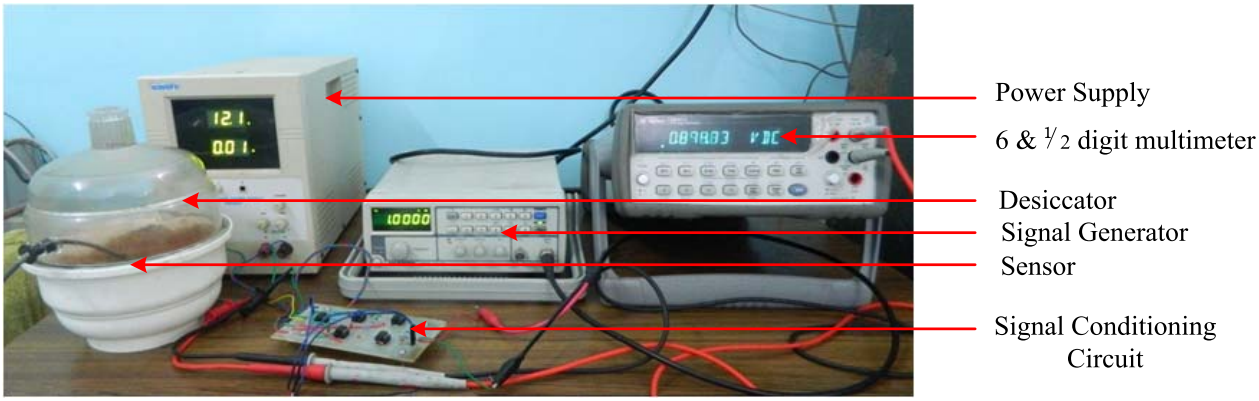

Fig. 11. Experimental laboratory setup for measuring soil moisture with a designed sensor.

TABLE V
REPEATABILITY CHECK OF THE SENSORS

Soil water content (W_w/W_s)	Model 1			Model 2			Model 3		
	Mean (pF)	St. Dev. (pF)	Max. Error (pF)	Mean (pF)	St. Dev. (pF)	Max. Error (pF)	Mean (pF)	St. Dev. (pF)	Max. Error (pF)
8.04%	377.62	3.23	4.79	276	2.09	3.7	602	6.30	9.2
16.08%	834.5	6.82	10.5	526	4.36	5.6	1425	10.02	18
20.46%	1205	9.46	12	677	8.70	12	1965	9.65	14
31.03%	1648	12.28	16	884	11.63	13	2780	13.83	20

is measuring the difference in the amplitude of the two waveforms. As there was some phase difference between the two signals at the test points, the signals were fed to two different peak detector circuits. A schematic of the basic peak detector circuit is shown in Fig. 10 [34].

The dc voltages of the two peak detectors were used on the inputs of a subtractor, and the difference was measured by a digital multimeter (DMM). The output voltage of the system is given by the equation as follows:

$$V_{\text{out}} = \frac{a(bC_s - 1)}{a^2C_s + abC_s + b + a} V_{\text{in}(p)} \tag{3}$$

where $a = 2\pi f R$, R is the resistance used in the bridge ($R1 = R2 = R$); $b = 1/C$, C is the standard capacitor; $V_{\text{in}(p)}$ is the peak voltage of the excitation signal of the bridge; and C_s is the capacitance of the soil moisture sensor.

E. Soil Sample Preparation

Four soil samples were acquired from different locations whose global positioning system locations are indicated in Table II. These samples were collected from a depth of 10 cm and grounded to a powder form. Two samples of clay soil and two samples of sandy soil were considered for the experiments, since both have a different water-holding capacity. The samples were prepared in the standard D4959-00 of the American Society for Testing and Materials International [3]. The collected soil samples were oven-dried at 150 °C and the drying was continued until there was no change in the weight of the samples. The samples were analyzed by the sequential X-ray fluorescence spectrometer PANalytical AXIOS to find their chemical compositions. The results are presented in Table III. The samples A and B are clay soil and samples C and D are sandy soil.

TABLE VI
COEFFICIENTS OF EQUATIONS OBTAINED FROM EXPONENTIAL FITTING

Co-efficients	Model 1	Model 2	Model 3
$\mathbf{Y_0}$	0.64959	0.43351	0.8113
A	-0.63442	-0.43388	-0.76284
$\mathbf{R_0}$	-0.06038	-0.06269	-0.08087
$\mathbf{R^2}$	0.99234	0.99029	0.97807

F. Experimental Setup

The experimental arrangement is shown in Fig. 11. The prepared sample was kept in a desiccator without any desiccant, only to prevent moisture loss through the evaporation of the sample during the test. The designed sensor was inserted deep into the soil sample. The capacitance output of the sensor was measured by an S-928 Systronics auto *LCR*-Q tester. To measure the sensor response, the sensor was connected to the signal conditioning circuit, and the voltage output was measured by a 61/2 digit digital multimeter Agilent 34401A.

III. EXPERIMENTAL RESULTS

The capacitance of the designed sensors in air (at 61% relative humidity) was measured as 95, 104, and 190.4 pF for Models 1–3, respectively. The standard for testing the sensors was prepared by following the gravimetric method. The capacitance variation of the sensors with soil moisture for soil sample A is shown in Fig. 12(a). Table IV clearly indicates that Model 3 has a higher sensitivity, and Model 2 has the better goodness of fit for linear straight-line fitting. Fig. 12(b) also indicates the same result of capacitance variation for the three sensors for soil sample B. Model 3 had the highest area of influence due to the presence of water in the soil as the

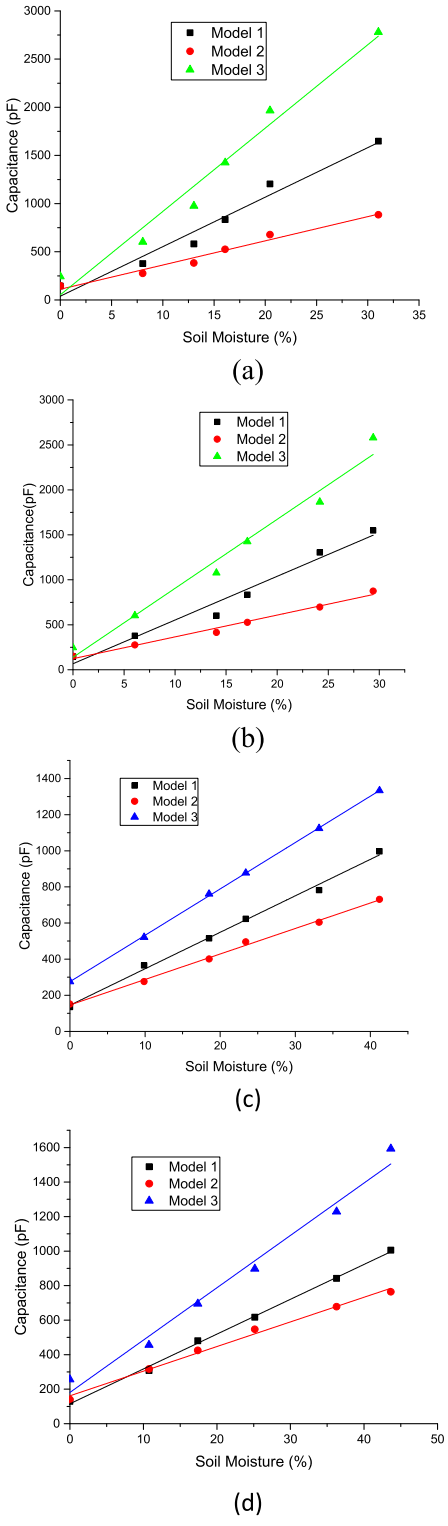

Fig. 12. Capacitance variation in soil samples. (a) Sample A. (b) Sample B. (c) Sample C. (d) Sample D.

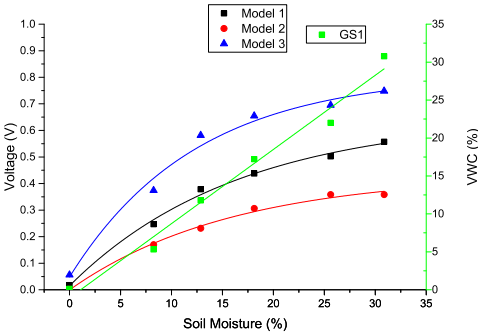

Fig. 13. Response of the system to soil moisture.

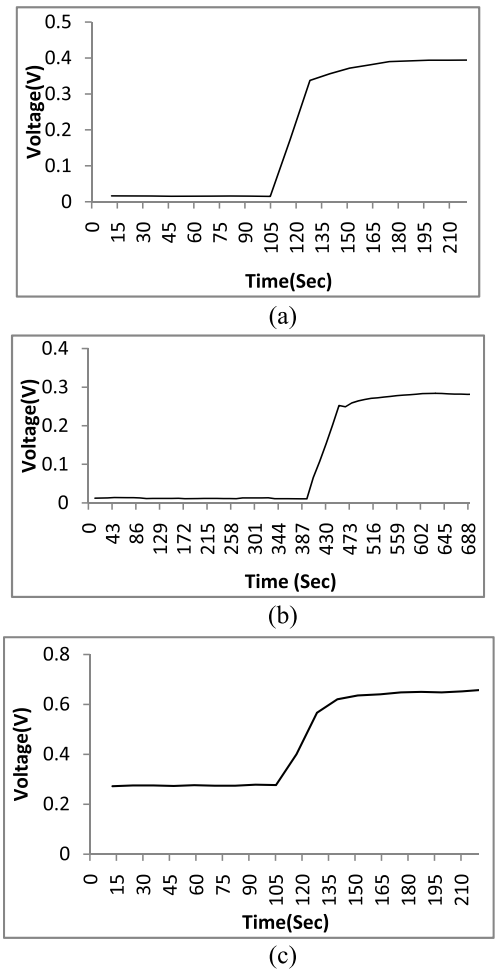

Fig. 14. Dynamic test for (a) Model 1, (b) Model 2, and (c) Model 3.

electrodes were fabricated on both the sides of the FR4 board and exposed to the soil. Hence, it had better sensitivity to the soil moisture variation. Model 1 had electrodes fabricated on one side of the FR4 board and this resulted in a lower sensitivity than Model 3. The continuous copper on the other side of the electrodes in Model 2 minimized the influence of water on the back side of the sensor, making it less sensitive to the change in soil moisture.

To check the repeatability of the sensors, four test setups were prepared with sample A at soil moisture 8.04%, 16.08%, 20.46%, and 31.03% and the sensor response of the three configurations were recorded at different times. The result, displayed in Table V, gives the mean value of the sensor response with standard deviations at different soil moistures. The maximum error from the mean value was also calculated. The maximum error for Model 1 was 1.27% of the mean value, whereas for Models 2 and 3, this was 1.77% and 1.518%, respectively.

TABLE VII
COMPARISON OF THE SENSORS WITH EXISTING SENSORS

Reported paper	Name of the sensor	Dimensions of the sensor (Heightx Width)	Copper trace's width	Distance between two copper traces	Number of copper traces	Results	Description of the sensor	Remarks
J. Mizuguchi et.al[26]	Sensor 1	10 cm x 20 cm	10 mm	0.4 mm	-	Capacitance variation is 20% for 2.7 ml water variation on the sensor surface	The backside of the sensing surface of the sensor is covered by copper layer and maintained in reference potential	The sensor is tested by adding water drops to the sensor surface and compared with a simulation result
	Sensor 2	236 mm x 67 mm	1.25 mm	0.35 mm	128	Variation in T_{th}(ms) to change in soil water content	The backside of the sensing surface of the sensor is covered by copper layer and maintained in reference potential	Capacitance change is measured in terms of time for a change in soil water content
R. N. Dean[24]	Prototype sensor 1	25.4 mm x 25.4 mm	152.4 µm	152.4 µm	70	Variation of capacitance from 63.9 pF to 321.3 pF as the sensor is inserted into water from air	The backside of the sensing surface has a solid layer of solder mask	Water is added to the sensor surface in weight and capacitance change is recorded
	Prototype sensor 2	83.8 mm x 26.7 mm	152.4 µm	152.4 µm	29	Capacitance variation from 20 pF to 100 pF for a variation of water content of soil from 0% to 33%	The backside of the sensing surface of the sensor is covered by copper layer and kept floating	Sensor response is recorded for a clay soil sample
As reported in this paper	Model 1	150 mm x 4.5 mm	2 mm	0.9 mm	51	Capacitance variation is recorded for four soil samples	The backside of the sensing surface has a solid layer of solder mask	Sensor response is recorded with clay and sandy soil samples
	Model 2	150 mm x 4.5 mm	2 mm	0.9 mm	51	Capacitance variation is recorded for four soil samples	The backside of the sensing surface of the sensor is covered by copper layer and kept floating	Sensor response is recorded with clay and sandy soil samples
	Model 3	150 mm x 4.5 mm	2 mm	0.9 mm	102	Capacitance variation is recorded for four soil samples	Both sides of the sensor have sensing parts with the same number of electrodes	Sensor response is recorded with clay and sandy soil samples

The voltage response of the system was measured by the DMM at intervals of 1 min, and the average voltage was used for the graph shown in Fig. 13. The voltage response of the sensors was nonlinear. After an exponential fitting for an equation, the resulting coefficients of the equations and goodness of fit (R^2) for the three designs are shown in Table VI. The nonlinear response of the output voltage with soil moisture for the developed sensing system is governed by (3). The volumetric water content was measured by the GS1 soil moisture probe of Decagon Devices and is also depicted with respect to the soil moisture measured by the thermogravimetric method in Fig. 13 to realize the behavior of the sensors. The output of the GS1 soil moisture sensor showed almost the same result as obtained by the thermogravimetric method and had a linear relationship with the gravimetric water content of the soil sample.

Dynamic test for the sensors was performed for sample A at 18.6% soil moisture of the sample and it showed that in comparison with Models 1 and 3, Model 2 was responding slowly to the change in the soil moisture. For this test, the sensor exposed to the ambient condition was inserted into the medium and the continuous data recording was switched ON. The response time was calculated from the recorded data as 22, 54, and 24 s for Models 1–3, respectively, as shown in Fig. 14.

Fringing field capacitive sensors fabricated on PCB, which were reported earlier, are compared with the sensors reported in this paper, as shown in Table VII. Models 1 and 2 discussed in this paper are the replica of prototype sensors with different dimensions reported earlier and tested with four different soil samples.

Numerous error sources may adversely affect the response of this type of sensors. The temperature effect and exposure of the interdigital electrodes to moisture for a long time may change the output of the sensors. To reduce the possibility of the error occurring from these two sources, the Kapton film can be used as an insulating medium for its high thermal stability and hydrophilic nature [29]. The selection of an optimal PCB for sensor fabrication will also help to reduce these types of errors in the sensor design. The careful measurement and application of the sensors minimize the possibility of errors. In view of the nonhomogeneous nature of soils, better results can be obtained if sensors are investigated with more number of soil samples.

IV. Conclusion

Three fringing field capacitive soil moisture sensors, two of which were proposed and used in different applications by different researchers earlier, were simulated, fabricated, and characterized. The fringing field technique was implemented on an FR4 copper clad board by using the PCB technology. The number of electrodes arranged in the interpenetrating comb pattern, fabricated on one side of the FR4 board, was designated as Model 1. Model 2 was having copper cladding on one side of the FR4 board and an interpenetrating comb pattern of electrodes on the other side. Model 3 was the novel configuration with the same electrodes on both the sides of an FR4 board. It was found that the sensitivity of the sensors changes with the change in the soil type, irrespective of the chemical compositions. It was also observed that Model 3 had a sensitivity higher than Models 1 and 2. Repeatability test showed the maximum error of 1.27%, 1.77%, and 1.518% of the mean value for Models 1–3, respectively. The dynamic test showed that Model 1 had a better response time of 22 s, which is followed by Model 3 with a response time of 24 s and Model 2 with a response time of 54 s. Model 3, which is a novel configuration, can replace conventional soil moisture sensors for the purpose of real-time soil moisture measurement as it has a higher sensitivity, a greater sensing area, and a better response time. As the design is simple and easily fabricated, these sensors can be fabricated with a minimum setup and within a limited cost. Signal conditioning electronics can be placed adjacent to the actual sensing electrodes; hence, the stray capacitance effect becomes minimum.

Acknowledgment

The authors would like to thank the Department of Science and Technology, Government of India, for providing the INSPIRE fellowship to one of the authors. They would like to thank the Department of Instrumentation and USIC, Gauhati University, Guwahati, India, for providing the necessary facilities to carry out the work and the SAIF, Department of Instrumentation, and USIC, Gauhati University. They would also like to thank Prof. P. K. Boruah, Professor (Retired) of Instrumentation and USIC, and Prof. J. Tamuli, Professor of Linguistics, for the encouragement and overall support.

References

[1] S. U. S. Lekshmi, D. N. Singh, and M. S. Baghini, "A critical review of soil moisture measurement," *Measurement*, vol. 54, pp. 92–105, Aug. 2014, doi: 10.1016/j.measurement.2014.04.007.

[2] P. A. C. Raats and M. T. Van Genuchten, "Milestones in soil physics," *Soil Sci.*, vol. 171, pp. S21–S28, May 2006. [Online]. Available: http://10.1097/01.ss.0000228048.85215.bf

[3] *Standard Test Method for Determination of Water Content of Soil by Direct Heating*, Standard ASTM D4959, West Conshohocken, PA, USA, 2000, doi: 10.1520/D4959-00.

[4] K. H. Tan, B. F. Hajek, and I. Barshad, "Thermal analysis techniques," in *Methods of Soil Analysis: Part 1—Physical and Mineralogical Methods*, vol. 9, A. Klute, Ed., 2nd ed. Madison, WI, USA: America Socirty Agronomy—Soil Science Society America, 1986, pp. 154–183.

[5] J. Ledieu, P. De Ridder, P. De Clerck, and S. Dautrebande, "A method of measuring soil moisture by time-domain reflectometry," *J. Hydrol.*, vol. 88, nos. 3–4, pp. 319–328, Nov. 1986, doi: 10.1016/0022-1694(86)90097-1.

[6] M. A. Hilhorst, "A pore water conductivity sensor," *Soil Sci. Soc. Amer. J.*, vol. 64, pp. 1922–1925, Nov. 2000, doi: 10.2136/sssaj2000.6461922x.

[7] B. Rao and D. N. Singh, "Moisture content determination by TDR and capacitance techniques: A comparative study," *Int. J. Earth Sci. Eng.*, vol. 4, no. 6, pp. 132–137, 2011. [Online]. Available: https://www.researchgate.net/profile/Devendra_Singh32/publication/264880333

[8] J. A. Huisman, S. S. Hubbard, J. D. Redman, and A. P. Annan, "Measuring soil water content with ground penetrating radar: A review," *Vadose Zone J.*, vol. 2, pp. 476–491, Mar. 2003, doi: 10.2113/2.4.476.

[9] T. Jackson, K. Mansfield, M. Saafi, T. Colman, and P. Romine, "Measuring soil temperature and moisture using wireless MEMS sensors," *Measurement*, vol. 41, no. 4, pp. 381–390, May 2008, doi: 10.1016/j.measurement.2007.02.009.

[10] J. Liu, M. Agarwal, K. Varahramyan, E. S. Berney, IV, and W. D. Hodo, "Polymer-based microsensor for soil moisture measurement," *Sens. Actuators B, Chem.*, vol. 129, no. 2, pp. 599–604, Feb. 2008, doi: 10.1016/j.snb.2007.09.017.

[11] K. Noborio, K. J. McInnes, and J. L. Heilman, "Measurements of soil water content, heat capacity, and thermal conductivity with a single TDR probe," *Soil Science*, vol. 161, no. 1, pp. 22–28, 1996, doi: 10.1097/00010694-199601000-00004.

[12] M. T. Julie and M. H. Jay, "Measuring soil water content in the laboratory and field with dual-probe heat-capacity sensors," *Agronomy J.*, vol. 89, no. 4, pp. 535–542, 1996, doi: 10.2134/agronj1997.00021962008900040001x.

[13] S. K. Vanapalli, D. G. Fredlund, and D. E. Pufahl, "The influence of soil structure and stress history on the soil–water characteristics of a compacted till," *Géotechnique*, vol. 49, no. 2, pp. 143–159, 1999, doi: 10.1680/geot.1999.49.2.143.

[14] D. N. Singh and S. J. Kuriyan, "Estimation of unsaturated hydraulic conductivity using soil suction measurements obtained by an insertion tensiometer," *Can. Geotech. J.*, vol. 40, no. 2, pp. 476–483, 2003, doi: 10.1139/t02-112.

[15] R. S. Alessi and L. Prunty, "Soil-water determination using fiber optics," *Soil Sci. Soc. Amer. J.*, vol. 50, no. 4, pp. 860–863, 1985, doi: 10.2136/sssaj1986.03615995005000040006x.

[16] A. L. Kaleita, L. F. Tian, and M. C. Hirschi, "Relationship between soil moisture content and soil surface reflectance," *Trans. ASAE*, vol. 48, no. 5, pp. 1979–1986, 2005. [Online]. Available: https://lib.dr.iastate.edu/cgi/viewcontent.cgi?article=1570&context=abe_eng_pubs

[17] R. K. Sharma and A. K. Gupta, "Continuous wave acoustic method for determination of moisture content in agricultural soil," *Comput. Electron. Agriculture*, vol. 73, no. 2, pp. 105–111, Aug. 2010, doi: 10.1016/j.compag.2010.06.002.

[18] Z. Yin, T. Lei, Q. Yan, Z. Chen, and Y. Dong, "A near-infrared reflectance sensor for soil surface moisture measurement," *Comput. Electron. Agriculture*, vol. 99, pp. 101–107, Nov. 2013, doi: 10.1016/j.compag.2013.08.029.

[19] P. C. Dias, W. Roque, E. C. Ferreira, and J. A. S. Dias, "A high sensitivity single-probe heat pulse soil moisture sensor based on a single *npn* junction transistor," *Comput. Electron. Agriculture*, vol. 96, pp. 139–147, Aug. 2013, doi: 10.1016/j.compag.2013.05.003.

[20] A. M. Thomas, "*In situ* measurement of moisture in soil and similar substances by 'fringe' capacitance," *J. Sci. Instrum.*, vol. 43, no. 1, p. 21, 1966. [Online]. Available: http://iopscience.iop.org/0950-7671/43/1/306

[21] H. Eller and A. Denoth, "A capacitive soil moisture sensor," *J. Hydrol.*, vol. 185, nos. 1–4, pp. 137–146, Nov. 1996, doi: 10.1016/0022-1694(95)03003-4.

[22] J. P. Bell, T. J. Dean, and M. G. Hodnett, "Soil moisture measurement by an improved capacitance technique, part II. Field techniques, evaluation and calibration," *J. Hydrol.*, vol. 93, nos. 1–2, pp. 79–90, Aug. 1987, doi: 10.1016/0022-1694(87)90195-8.

[23] S. G. Ungar, R. Layman, J. E. Campbell, J. Walsh, and H. J. McKim, "Determination of soil moisture distribution from impedance and gravimetric measurements," *J. Geophys. Res.*, vol. 97, no. D17, pp. 18969–18977, Nov. 1992, doi: 10.1029/92JD01450.

[24] R. N. Dean, A. Rane, M. Baginski, Z. Hartzog, and D. J. Elton, "Capacitive fringing field sensors in printed circuit board technology," in *Proc. IEEE Instrum. Meas. Technol. Conf.*, Austin, TX, USA, May 2010, pp. 970–974, doi: 10.1109/IMTC.2010.5488058.

[25] V. Markevicius, D. Navikas, A. Valinevicius, D. Andriukaitis, and M. Cepenas, "The soil moisture content determination using interdigital sensor," *Elektron. Elektrotechnika*, vol. 18, no. 10, pp. 25–28, 2012, doi: 10.5755/j01.eee.18.10.3055.

[26] J. Mizuguchi, J. C. Piai, J. A. de França, M. B. de Morais França, K. Yamashita, and L. C. Mathias, "Fringing field capacitive sensor for measuring soil water content: Design, manufacture, and testing," *IEEE Trans. Instrum. Meas.*, vol. 64, no. 1, pp. 212–220, Jan. 2015, doi: 10.1109/TIM.2014.2335911.

[27] K. Chetpattananondh, T. Tapoanoi, P. Phukpattaranont, and N. Jindapetch, "A self-calibration water level measurement using an interdigital capacitive sensor," *Sens. Actuators A, Phys.*, vol. 209, pp. 175–182, Mar. 2014, doi: 10.1016/j.sna.2014.01.040.

[28] R. B. McIntosh and M. E. Casada, "Fringing field capacitance sensor for measuring the moisture content of agricultural commodities," *IEEE Sensors J.*, vol. 8, no. 3, pp. 240–247, Mar. 2008, doi: 10.1109/JSEN.2007.913140.

[29] A. Fuchs, M. J. Moser, H. Zangl, and T. Bretterklieber, "Using capacitive sensing to determine the moisture content of wood pellets–investigations and application," *Int. J. Smart Sens. Intell. Syst.*, vol. 2, no. 4, pp. 293–308, 2009, doi: 10.21307/ijssis-2017-352.

[30] M. S. A. Rahman, S. C. Mukhopadhyay, and P.-L. Yu, "Novel planar interdigital sensors," in *Novel Sensors for Food Inspection: Modelling, Fabrication and Experimentation*, vol. 10. Cham, Switzerland: Springer, Jan. 2014, pp. 11–35, doi: 10.1007/978-3-319-04274-9_2.

[31] E. F. da Costa *et al.*, "A self-powered and autonomous fringing field capacitive sensor integrated into a micro sprinkler spinner to measure soil water content," *Sensors*, vol. 17, no. 3, p. 575, 2017, doi: 10.3390/s17030575.

[32] A. V. Mamishev, K. Sundara-Rajan, F. Yang, Y. Du, and M. Zahn, "Interdigital sensors and transducers," *Proc. IEEE*, vol. 92, no. 5, pp. 808–845, May 2004, doi: 10.1109/JPROC.2004.826603.

[33] A. Heidary and G. C. M. Meijer, "An integrated interface for leaky capacitive sensor with emphasize on humidity sensor," in *Proc. IEEE IMTC*, Victoria, BC, Canada, May 2008, pp. 1613–1616, doi: 10.1109/IMTC.2008.4547301.

[34] K. Kalita, N. Das, P. K. Boruah, and U. Sarma, "Development of a strain measurement system for the study of effect of relative humidity on wood," *Measurement*, vol. 94, pp. 265–272, Dec. 2016, doi: 10.1016/j.measurement.2016.08.001.

Manash Protim Goswami received the master's degree in instrumentation from Gauhati University, Guwahati, India, in 2011, where he is currently pursuing the Ph.D. degree with the Department of Instrumentation and USIC.

His current research interests include advanced instrumentation for precision horticulture, sensor development, and embedded system design.

Babak Montazer received the M.Sc. degree in electronics from the University of Pune, Pune, India, in 2011. He is currently pursuing the Ph.D. degree with the Department of Instrumentation and USIC, Gauhati University, Guwahati, India.

His current research interests include the investigation and characterization of piezoelectric MEMS transducers for energy harvesting device and sensor development.

Utpal Sarma (M'14) received the M.Sc. degree in physics and the Ph.D. degree from Gauhati University, Guwahati, India, in 1998 and 2010, respectively.

In 1999, he joined the Department of Physics, B. Borooah College, Guwahati, as a Lecturer. In 2007, he joined Gauhati University as an Assistant Professor, where he is currently a Professor. His current research interests include embedded system for agro industries, sensor instrumentation, and microenergy harvesting devices.